Conference Paper, Published Version

Okamoto, Takaaki; Nezu, Iehisa

Flow resistance law in open-channel flows with rigid and flexible vegetation

River Flow 2010 - Dittrich, Koll, Aberle & Geisenhainer (eds) - © 2010 Bundesanstalt für Wasserbau ISBN 978-3-939230-00-7

Flow resistance law in open-channel flows with rigid and flexible vegetation

Taka-aki Okamoto & Iehisa Nezu
Department of Civil Engineering, Kyoto University, Kyoto 615-8540, Japan

ABSTRACT: A lot of aquatic plants are observed in actual rivers and they have a potential to improve water quality. A large-scale coherent vortex is generated near the vegetation edge, which dominate the momentum and scalar transport. Thus, estimating the flow resistance of vegetated flows is of great importance in river management. In such vegetated open-channel flows, both the geometry of the vegetation elements (shape, size, flexibility and vegetation density) and turbulence characteristics affect the hydrodynamic resistance significantly. However, any important relation between the vegetation motion and the flow resistance property is not yet established. Therefore, in the present study, we highlighted these important topics and measured the instantaneous velocity structure and coherent motion in open-channel flows with flexible vegetation by using PIV technique. As the results, the hydro-mechanic interaction between the flow and flexible plant motion was revealed.

Keywords: Flow resistance, Flexible vegetation, Plant motion, PIV

1 INTRODUCTION

Aquatic plants are fundamental components of a natural water environment, and the current environmental river management prefers to preserve natural wetland and floodplain vegetation, although a lot of aquatic plants have been removed to prevent water disaster in actual rivers. A large-scale coherent vortex is generated near the vegetation edge, which dominate the momentum and scalar transport between the over- and within vegetation. Thus, estimating the flow resistance of vegetated flows is of great importance in river management. In such vegetated open-channel flows, both the geometry of the vegetation elements (shape, size, flexibility and vegetation density) and turbulence characteristics will affect the hydrodynamic resistance significantly.

Kouwen & Unny (1973) conducted the earlier experiments of flexible vegetated open-channel flows by Pitot tube. The log-law distribution described well the velocity profile above the vegetation layer.

Jarvela (2002) investigated the flow resistance of the flexible and stiff vegetation in a laboratory flume. They revealed that the friction factor was dependent mostly on the deflected height of flexible vegetation, the flow velocity and water depth.

Stephan & Gutknecht (2002) conducted the velocity measurements above the flexible vegetation by acoustic Doppler velocimetry (ADV) to determine the relationship between the hydraulic roughness and the deflected height of vegetations. The analysis of the velocity measurements showed that the zero plane displacement of the logarithmic law was correlated with the deflected plant height.

Velasco et al. (2003) have investigated a hydro-mechanical interaction between the flow and flexible plants by using ADV, and found some interesting relations between the flow field and the local plant deformation.

Carollo et al. (2005) pointed out that the application of Kouwen‘s method produces a systematical overestimation of flow resistance in natural flexible vegetation flow. To obtain good agreement with experimental data, the coefficients appearing in the log-law type flow resistance were re-estimated.

Nikora et al. (2008) examined the effects of aquatic vegetation on hydraulic properties in a range of vegetation types and their characteristic patch patterns. They suggested simple qualitative relationships to predict these effects using the vegetation parameters. Comparisons among the vegetation parameters indicated that the submergence depth ratio was the best parameter for roughness.

Righetti (2008) investigated the mean flow and turbulence structure in an open-channel flow with flexible vegetation by using a 3-D ADV. They conducted the *time- averaging* and *space-*

Table1 Hydraulic condition

Type	a (1/m)	H (cm)	h (cm)	H/h	U_m (cm/s)	Re	Fr	Classification of plant motion
R	7.6	15.0	5.0	3.0	10.0	15000	0.08	**Rigid(R)**
					12.0	18000	0.10	
					15.0	22500	0.12	
					17.0	25500	0.14	
					20.0	30000	0.16	
					25.0	37500	0.21	
F5					10.0	15000	0.08	**Swaying(S)**
					12.0	18000	0.10	
					15.0	22500	0.12	
					17.0	25500	0.14	
					20.0	30000	0.16	
					25.0	37500	0.21	**Monami(M)**
					30.0	45000	0.25	
					35.0	52500	0.29	
F7		21.0	7.0		10.0	21000	0.07	**Swaying(S)**
					12.0	25200	0.08	
					15.0	31500	0.10	**Monami(M)**
					17.0	35700	0.12	
					20.0	42000	0.14	
					25.0	52500	0.17	
					30.0	63000	0.21	
					35.0	73500	0.24	
F9		27.0	9.0		10.0	27000	0.06	**Swaying(S)**
					12.0	32400	0.07	
					15.0	40500	0.09	**Monami(M)**
					17.0	45900	0.10	
					20.0	54000	0.12	
					25.0	67500	0.15	
F10.5		31.5	10.5		10.0	31500	0.06	**Swaying(S)**
					12.0	37800	0.07	
					15.0	47250	0.09	**Monami(M)**
					17.0	53550	0.10	
					20.0	63000	0.11	
					25.0	78750	0.14	

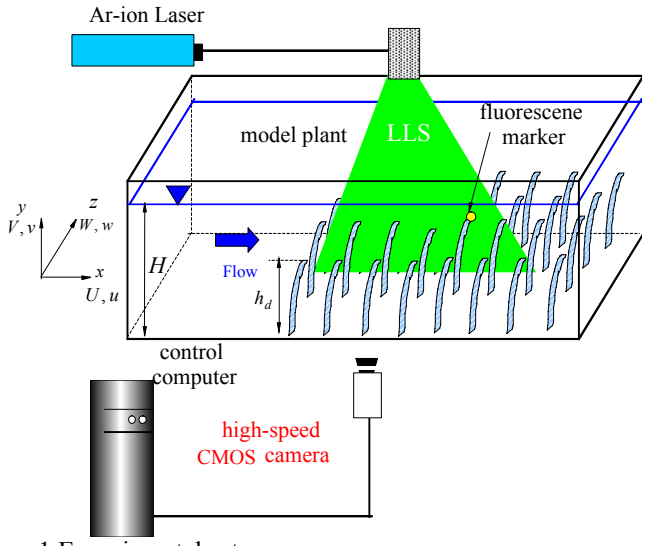

Figure 1 Experimental set-up

averaging (Double-averaging) method and revealed that the mean velocity, the vegetation density and the plant flexibility are the driving parameters for the developing of a mixing layer near the canopies.

Recently, Okamoto & Nezu (2009) have conducted the simultaneous measurements of turbulence and vegetation motion in open-channel flows with flexible vegetation by using a combination of PIV and PTV techniques. They examined the relation between coherent vortices and organized plant motion, so-called Monami phenomena.

These vegetated open-channel flows have received much attention in the past decades. However, in such vegetated open-channel flows, both the properties of vegetation elements and turbulence characteristics may affect the hydrodynamic resistance significantly. Therefore, in the present study, turbulence measurements were conducted for rigid and flexible vegetation flows by using PIV techniques. As the results, the characterization of flow resistance due to flexible vegetation roughness was examined by changing vegetation height.

2 EXPERIMENTAL METHOD

2.1 *Experimental setup and vegetation model*

Laboratory experiments were carried out in a 10-m long and 40cm wide tilting flume, as shown in Figure1. x, y and z are the streamwise, vertical and spanwise coordinates, respectively. The vertical origin, $y = 0$, was chosen on the channel bed. $\widetilde{u} \equiv U + u$, $\widetilde{v} \equiv V + v$ and $\widetilde{w} \equiv W + w$ are the instantaneous velocity components in each coordinate. U and V are the time-averaged velocity components for streamwise and vertical directions, respectively. u and v are the corresponding velocity fluctuations.

H is the water depth, h is the vegetation height and h_d is the deflected height of flexible vegetation. The rigid vegetation was modeled as rigid strip plates (h=50mm height, b=8mm width and t=1mm thickness) in the same manner as conducted in laboratory experiments by Nezu & Sanjou (2008). The present flexible vegetation elements were all the same and made of h=50, 70,

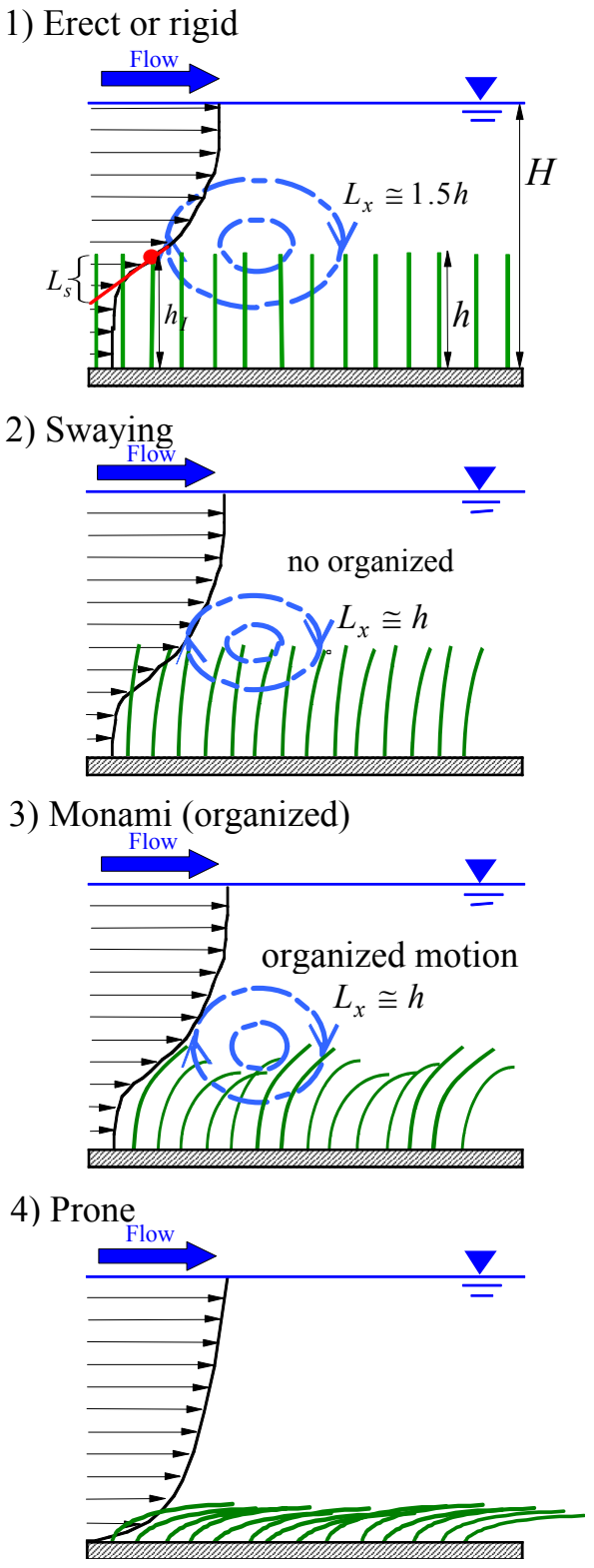

Figure 2 Flow patterns in dense flexible vegetation

90, 105mm height, b=8mm width and t=0.1mm thickness OHP film strip sheets. The flexural rigidity J ($=E\times I$) of this vegetation element was $J=7.3\times10^{-5}$ Nm^2 by preliminary experiments, in which E is the stiff modulus and I is the inertial moment of vegetation. The present value is in the same order of magnitude as $J=1.7\times10^{-5}$ Nm^2 of Velasco et al. (2003) for aquatic vegetation elements.

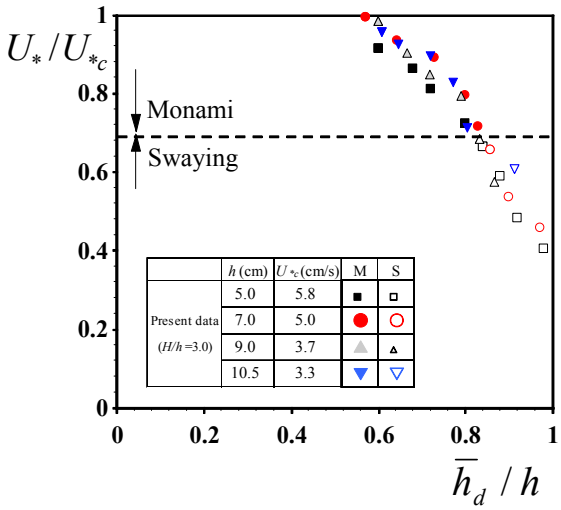

Figure 3 Classification of Swaying type and Monami type in flexible vegetation

In the present study, the instantaneous velocity components $(\tilde{u},\tilde{v})$ were calculated by PIV algorism, in which the fluid tracers were Nylon-12 particles of 100 μm diameter and 1.02 specific density. The illuminated flow pictures on the x-y plane were taken by a high-speed CMOS camera (1024×1024 pixels) with 500Hz frame rate and 60s sampling time. A laser light sheet (LLS) was projected into the water vertically from the free surface. The 2mm thickness LLS was generated by 3W Argon-ion laser using a cylindrical lens.

2.2 *Classification of vegetation motion*

Table 1 shows the hydraulic condition. Experiments were conducted for both rigid and flexible vegetations on the basis of six flow scenarios, in which the flexible vegetation height h was changed from 5.0cm to 10.5cm. However, the relative submergence depth H/h and the bulk mean velocity U_m were kept constant for all cases. The classification of plant motions is indicated in Table 1. ‘‘S’’ means *Gently Swaying (non-organized waving)*, and ‘‘M’’ means *Monami (organized waving)*.

The flexible vegetation motion was classified into four types on the basis of both the hydrodynamic action of the flow and the flexural rigidity EI. Four types have been observed experimentally in flexible vegetated flows, e.g., see Carollo et al. (2005) and Okamoto & Nezu (2009):

1. Vegetation elements are *Erect* and do not change their tip position in time
2. Vegetation elements are independently waving each other (*Gently Swaying*), i.e. without organized motions
3. Vegetation elements are deflected more significantly and the coherent waving motion of vegetation is observed (*Monami*)

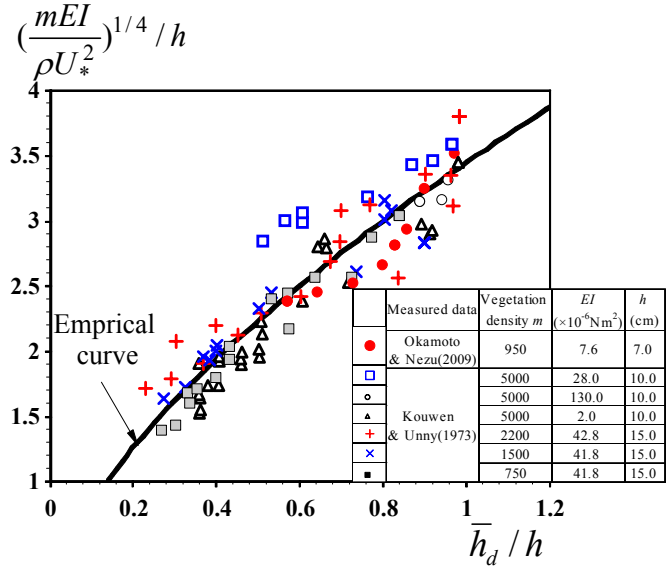

Figure 4 Relation between aggregate stiffness *mEI* and the deflection h_d

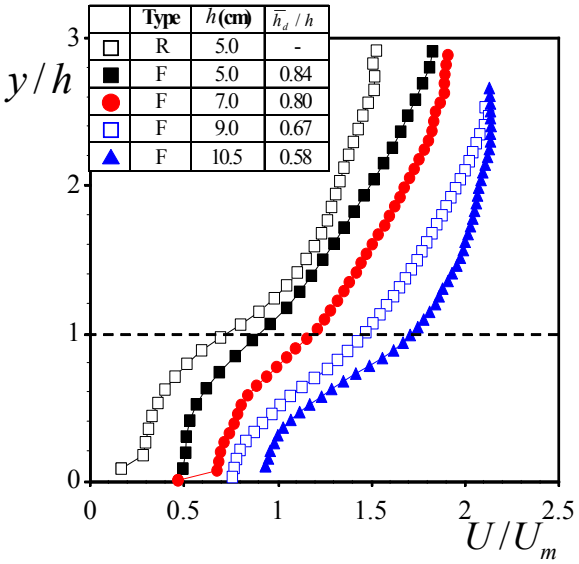

Figure 5 Mean velocity

4. Vegetation elements assume permanently a *Prone* position

Figure 2 schematizes the flexible vegetation motion patterns. The undeflected height h of a flexible vegetation element corresponds to the rigid vegetation height. In contrast, $\overline{h}_d$ is the time-averaged value of the fluctuating deflected height $h_d(t)$ of a typical flexible-vegetation element. In Type 1, the flexible vegetations assume a *Erect* behavior for low flow velocity. This *Erect* flow pattern is analogous to the 'Rigid' vegetated open-channel flows. In Types 2 and 3, the vegetation motion depends on the flow condition and the plant morphology. It is important to note that a shear-layer is generated only when the vegetation density increases above a threshold value and the momentum absorption by the canopies is sufficient to produce an inflection point in the velocity profile, which is needed to trigger *Monami* phenomena.

For low *EI* values and higher flow velocity, the flexible vegetation elements assume the *Prone* position. As the flexural rigidity *EI* increases, the higher values of flow velocity are necessary in order to reach the *Prone* type. Kouwen & Unny (1973) proposed that the flexible vegetation shows a *Prone* configuration when the friction velocity U_* is higher than a critical value U_{*C}. They found then that the value of U_{*C} is a function of the vegetation height h, the vegetation density a and the flexural rigidity J.

Figure 3 shows the variations of the friction velocity U_*/U_{*C} against the time-averaged deflected height $\overline{h}_d/h$ for the different flexible vegetation heights of h= 5.0, 7.0, 9.0, 10.5(cm). In this figure, the vegetation density a and the flexural rigidity *EI* of the flexible vegetations are kept constant (a=7.6(1/m), EI = 7.3×10^{-5} [Nm^2]). This figure shows that the larger friction velocity, i.e., the higher velocity, causes the deflection of plants more significantly, which is in good agreement with Kouwen & Unny (1973). Of particular significance is that the Monami occurs at $U_*/U_{*C} \geq$ say 0.75, whereas, the Swaying occurs at the lower friction velocity, i.e., the lower flow- resistance force. These results are interesting findings and should be further investigated in more detail.

3 RESULTS

3.1 Mean *flow*

Figure 4 shows the deflected flexible vegetation heigh $\overline{h}_d/h$ versus a non-dimensional parameter $\left(mEI/\rho U_*^2\right)^{1/4}/h$, in which m is the vegetation density used by Kouwen & Unny (1973). The values of $\overline{h}_d/h$ were obtained from PTV measured data by Okamoto & Nezu (2009). The present data are compared with those of Kouwen & Unny (1973). They evaluated the deflection of flexible vegetation elements by the use of the rigidity factor, *EI*. On the basis of experiments carried out in laboratory flume with flexible vegetation of six different patterns, Kouwen & Unny (1973) deduced the following empirical formula:

$$\frac{h_d}{h} = \frac{3.57}{h}\left(\frac{mEI}{\rho U_*^2}\right)^{1/4} - 0.286 \qquad (1)$$

The present data are in good agreement with Kouwen & Unny (1973)'s data and also with Eq.(1), although there are some scatters among data. Consequently, Eq.(1) of Kouwen & Unny (1973) may be used to evaluate the deflected vegetation height $\overline{h}_d$, which is necessary to consider the resistance law. Eq. (1) is written in the following form:

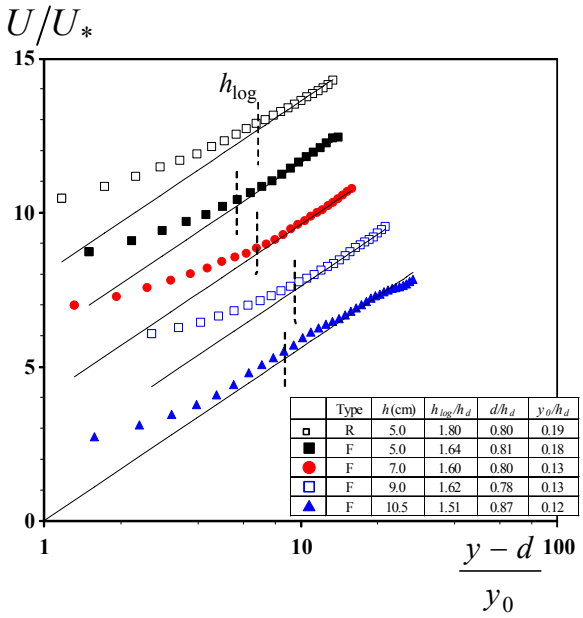

Figure 6 Semi-log plot of mean velocity over canopy

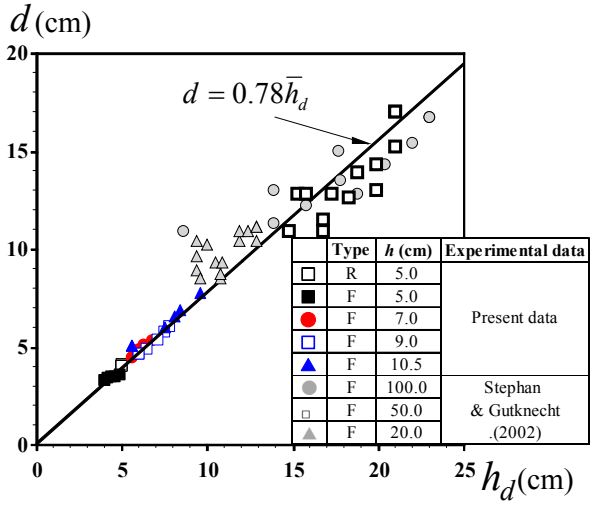

Figure 7 Zero-plane displacement

$$mEI = \frac{1}{3.57}\left(\bar{h}_d + 0.286h\right)^4 \rho U_*^2 \qquad (2)$$

For natural vegetation, the value of flexural rigidity EI may be estimated from (2) by measuring h, $\bar{h}_d$, m and U_*.

Figure 5 shows the mean velocity profiles $U(y)$ for different vegetation height. The values of U are normalized by the bulk mean velocity U_m. The values of U/U_m are shifted in the longitudinal axis by 0.2 units. The strong shear layer near the top of the canopy is produced and a significant inflection-point appears near the vegetation top (y=h for rigid canopy and y=$\bar{h}_d$ for flexible one), which is in good agreement with Nepf & Vivoni (2000).

The values of $\bar{h}_d/h$ are indicated in the legend of Figure 5. The flexible vegetation is deflected more significantly, as the plant height h increases. Consequently, the height of the inflection-point decreases with an increase of the vegetation length (or height) h.

Several researchers have pointed out that the velocity over the submerged canopy obeys the log-law profile of Eq.(3).

$$U/U_* = \frac{1}{\kappa}\ln\left(\frac{y-d}{y_0}\right) \qquad (3)$$

in which, d and y_0 are the zero-plane displacement thickness and the roughness height, respectively. Figure 6 shows the semi-log plot of the mean velocity U/U_* against the normalized coordinate $(y-d)/y_0$. The values of U/U_* are shifted upwards by 2 units. The friction velocity U_* was defined as the peak value of the Reynolds stress $-uv$.

It is observed that the mean velocity profile $U(y)$ obeys the log-law of Eq.(1) very well farther from the canopy edge. $h_{\log}$ is the lower limit position of the log-law zone, in which turbulence characteristics are more analogous to those of boundary layers rather than mixing-layers, as pointed out by Nezu & Sanjou (2008). The values of $h_{\log}/\bar{h}_d$ are almost constant of 1.6 for flexible vegetation, which is in the same order of magnitude as $h_{\log}/h = 1.8$ of Nezu & Sanjou (2008) for rigid vegetation.

The zero-plane displacement d corresponds to the mean level of momentum absorption, as follows:

$$d = \int_0^h \left(y\frac{\partial\overline{uv}}{\partial y}\right)dy \Big/ \int_0^h \left(\frac{\partial\overline{uv}}{\partial y}\right)dy \qquad (4)$$

Eq.(4) was also used in aquatic canopy flows by Nepf & & Vivoni (2000) and Nezu & Sanjou (2008). The roughness height y_0 was determined so that the experimental values of U/U_* might be best-fitted to the log-law of (3). Figure 7 shows the zero-plane displacement d, against the deflected vegetation height $\bar{h}_d$. The zero-plane displacement seems to be correlated well with the deflected plant height, resulting in d/h_d=0.78. This value is in good agreement with Stephan & Gutnecht (2002)'s data of d/h_d=0.83. The zero-plane displacement becomes larger with an increase of the vegetation length h.

The values of $y_0/\bar{h}_d$ are also indicated in the legend of Figure 6. As the averaged values, $y_0/\bar{h}_d$=0.14 was obtained for flexible vegetation. This value is consistent with Nepf & Vivoni(2000), who obtained y_0/h=0.11. These results suggest that the mean plant height $\bar{h}_d$ becomes an important parameter for describing the influence of roughness on the overall flow field.

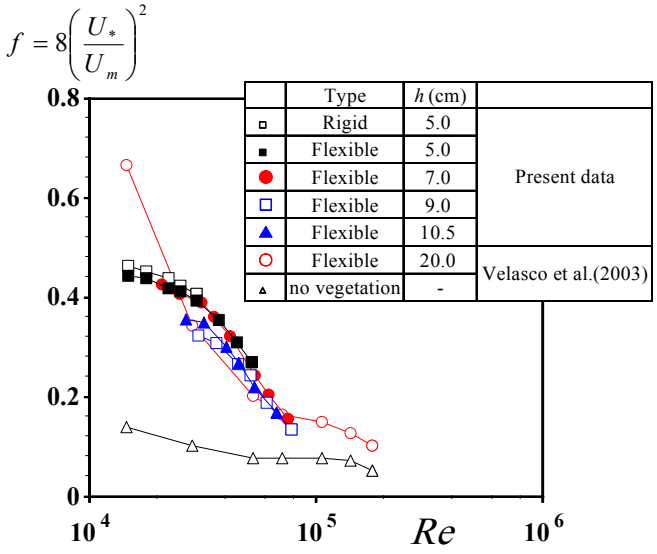

Figure 8 Friction factor f versus Re

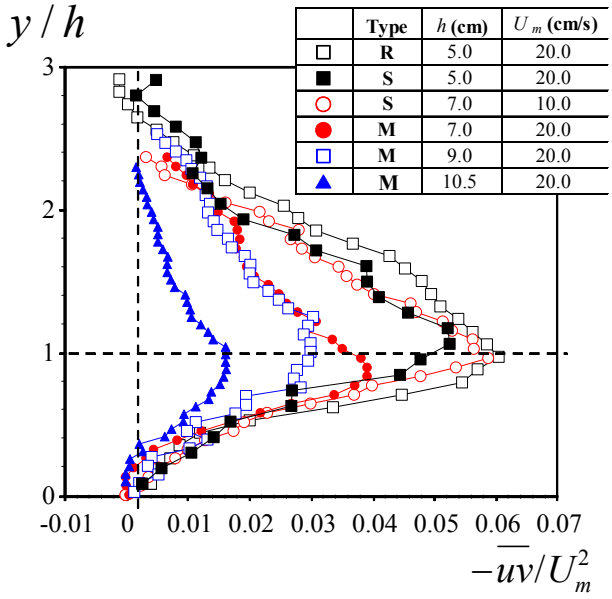

Figure 10 Reynolds stress distribution

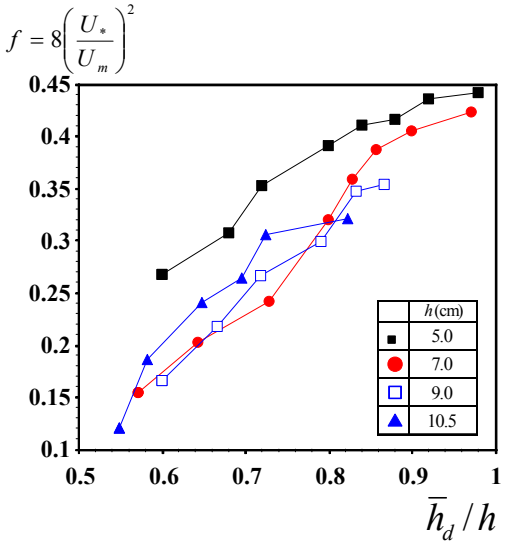

Figure 9 Friction factor f versus the deflected flexible vegetation height

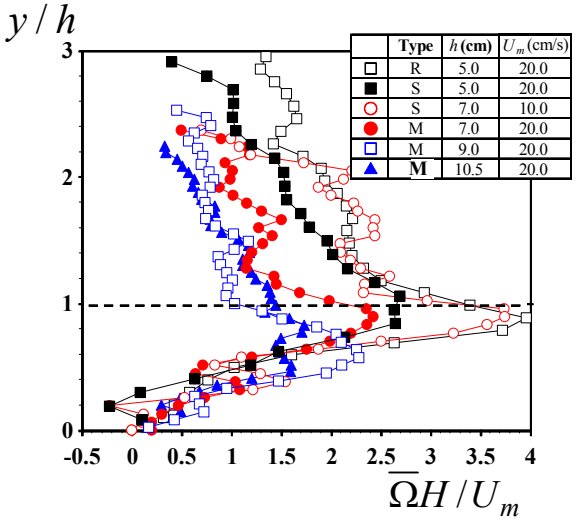

Figure 11 Vertical distribution of the time-averaged vorticity

3.2 *Flow resistance law*

The estimation of the friction factor is very important in river engineering. Figure8 shows the values of the friction factor $f = 8(U_* / U_m)^2$ of Darcy-Weisbach for Rigid and Flexible vegetations. For a comparison, the Flexible vegetation data of Velasco et al. (2003) are also included in Figure8. The friction factor f decreases as the Reynolds number Re increases. It is also observed that the values of f for flexible canopy are smaller than those for rigid canopy. This implies that the deflection of the flexible vegetation reduces the flow resistance.

Figure 9 shows the variations of the friction factor f against the time-averaged deflected height $\overline{h}_d / h$ for the different flexible vegetation length of h= 5.0, 7.0, 9.0, 10.5(cm). The friction factor f increases as the deflected height $\overline{h}_d / h$ becomes larger. These results are in good agreement with Jarvela (2002)'s data.

Kouwen & Unny (1973) suggested that the friction factor is a function of the deflected plant height $\overline{h}_d$ for 'Swaying' and 'Monami' canopies. In contrast, the flow boundary becomes a smooth wavy surface for the 'Prone' type flow. This 'Prone' canopy flow has not been fully investigated as yet.

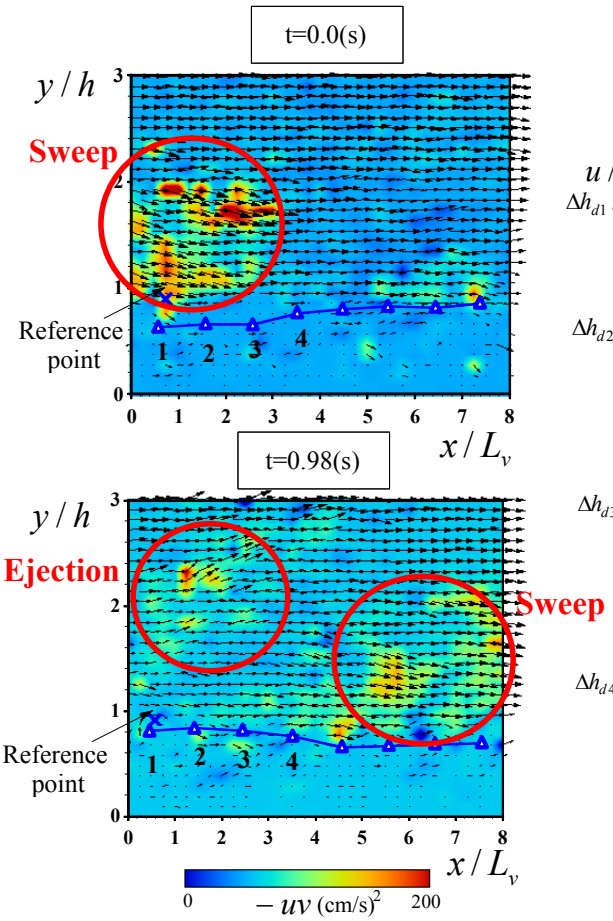

Figure 12 Instantaneous velocity vectors and vegetation motions for Monami

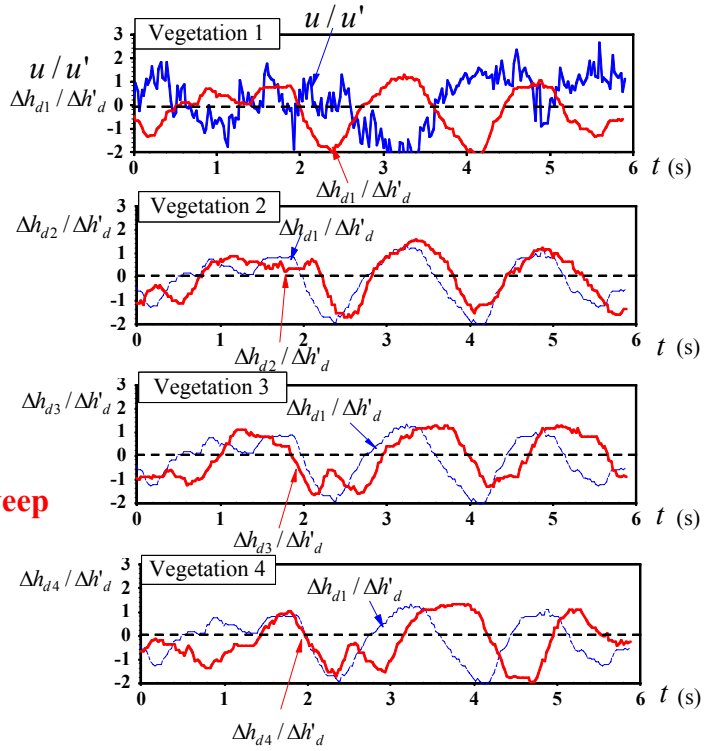

Figure 13 Time series of streamwise velocity $u(t)$ and the deflected-vegetation height, $h_d(t)$

3.3 *Turbulence structure*

Figure10 shows the vertical distribution of the Reynolds stress $-\overline{uv}$ normalized by the bulk mean velocity U_m for different height plant models. This ratio $-\overline{uv}/U_m^2$ is a measure of momentum exchange efficiency. The $-\overline{uv}$ distribution for Swaying (S) canopy is similar to that for Rigid (R) canopy one, which have a sharp peak near the vegetation edge (y/h=1.0).

In contrast, in the Monami canopy, the $-\overline{uv}$ has a milder peak structure. The peak values of $-\overline{uv}$ become smaller for Monami canopy than for Rigid canopy, which is consistent with the observation of Ghisalberti & Nepf (2006). This implies that for Rigid canopy, the strong shear layer near the vegetation edge generates a large-scale coherent vortex and the larger momentum is transported toward the within-canopy, as pointed out by Nezu & Sanjou (2008). In contrast, for Monami (M) canopies, the oscillations of flexible vegetation increase the momentum absorption near the canopy much higher compared to Rigid (R) canopies.

Figure 11 shows the vertical distribution of the time-averaged vorticity $\overline{\Omega}(y)$ for Rigid and Flexible vegetation flows. The corresponding instantaneous vorticity Ω is defined as

$$\Omega = \frac{\partial \tilde{v}}{\partial x} - \frac{\partial \tilde{u}}{\partial y} \tag{5}$$

$\overline{\Omega}(y)$ is a measure of the vortex rotation. The distributions of $\overline{\Omega}$ have the peak value near the vegetation edge. This indicates that the large-scale coherent vortices are generated at the vegetation edge. The values of $\overline{\Omega}$ for Rigid vegetation become lager than those for Flexible vegetation. Nepf & Ghisalberti (2008) also suggested that the Rigid canopy generates comparatively larger and more rapidly rotating vortices than the Flexible canopy.

Figure 10 and 11 indicate that the flexible vegetation elements are deflected significantly for Monami canopies and the coherent vortices become weaker and smaller. This conclusion is supported by the observed Reynolds stress distribution $-\overline{uv}/U_m^2$ shown in Figure10.

3.4 *Instantaneous structure*

PIV techniques are much more powerful to capture a whole velocity field and to examine the trajectory of the instantaneous coherent motion than point measurements such as LDA and ADV. Figure 12 shows some examples of the instantaneous

velocity vectors $(\tilde{u}, \tilde{v})$ for flexible canopy (h=7.0cm, Monami). The colored contour indicates the value of u. The tip positions $(\Delta x, \Delta y)$ of vegetations are also included by triangular symbols in Figure12.

At t=0.0s, the Sweep motion is observed above the vegetation edge and the flexible vegetations are deflected most significantly in the region of x/L_v = 1.0-4.0. At t=0.98s, the Sweep motion is followed by the Ejection motion and the instantaneous flexible vegetation height h_d(t) increases at x/L_v = 1.0-4.0.

Figure 13 shows the time-series of the streamwise velocity u(t) at the vegetation edge (y/h=1.0) and the flexible vegetation height h_d(t). The vegetation elements 1, 2, 3, 4 correspond to the flexible vegetations 1, 2, 3, 4 in Figure13. At t=0.0-0.5s, the flexible vegetations are deflected by the Sweep motion in Figure 12. At t=0.6-1.2s, the Ejection motion in Figure 13 appears near the vegetation edge and the instantaneous flexible vegetation height h_d(t) increases. It is also observed that the coherent waving motion of flexible plants is convected in the downstream. Figs. 12 and 13 show the periodical generation mechanism of sweeps and ejections for Monami canopy. These results are consistent with Okamoto & Nezu (2009).

4 CONCLUSIONS

In the present study, we highlighted these important topics and measured the instantaneous velocity structure and coherent motions in open-channel flows with flexible vegetations by using PIV technique. Furthermore, we revealed the hydro-mechanic interaction between flow and flexible plant motion.

The significant results obtained in this study are as follows:

1. We classified the flexible vegetation motion by using the critical friction velocity U_{*C}. The Monami occurs at the higher friction velocity ($U_* / U_{*C} \geq 0.75$), whereas the Swaying occurs at the lower friction velocity.
2. Mean velocity profile obeys the log-law very well farther from the canopy edge. The zero-plane displacement is correlated well with the deflected plant height. These results suggest that the mean deflected plant height becomes an important parameter for describing the influence of roughness in overall flow field.
3. The friction factor f increases as the deflected height becomes larger. It is also observed that the values of f for flexible canopy are smaller than those for rigid canopy.
4. The flexible vegetation elements are deflected significantly for Monami canopies and the coherent vortices near the vegetation edge become weaker and smaller.

REFERENCES

Carollo, F.G., Ferro, V. and Termini, D. 2005. Flow Resistance Law in Channels with Flexible Submerged Vegetation, J. of Hydr. Eng.,131, 554-564

Ghisalberti, M. and Nepf, H. 2006. The structure of the shear layer in flows over rigid and flexible canopies, Environ. Fluid Mech., 6, 277-301.

Jarvela, J. 2002. Flow resistance of flexible and stiff vegetation: flume study with natural plants, J. of Hydrology. 269. 44-54

Kouwen, N. and Unny, T.E. 1973. Flexible roughness in open-channels. ASCE J. Hydraulics Div. 99(HY5), 713-727.

Nepf, H. M. and Ghisalberti, M. 2008. Flow and transport in channels with submerged vegetation, Acta Geophysica, 80, 99-128.

Nepf, H., and Vivoni, E. R. 2000. Flow structure in depth-limited vegetated flow, J. of Geophys. Res.105, 28547-28557.

Nezu, I., and Sanjou. M. 2008. Turbulence structure and coherent motion in vegetated canopy open-channel flows, J. of Hydro-environment Res., IAHR, 2, 62-90.

Nikora, V., Lamed, S., Nikora, N., Debnath, K., Cooper, G. and Reid, M. 2008. Hydraulic resistance due to aquatic vegetation in small streams: field study, J. of Hydraulic Engineering, 134(9), 1326-1332

Okamoto, T. and Nezu, I. 2009. Turbulence structure and "Monami'' phenomena in flexible vegetated open-channel flows, J. of Hydraulic Res., Vol.47, pp.798-810

Righetti, M. 2008. Flow analysis in a channel with flexible vegetation using double-averaging method, Acta Geophysica., 56, 801-823.

Stephan, U. and Gutkcht D. 2002. Hydraulic resistance of submerged flexible vegetation, J. of Hydrology, 269, 27-43

Velasco, D., Bateman, A. Redondo, J. and Demedina, V. 2003. An open channel flow experimental and theoretical study of resistance and turbulent characterization over flexible vegetated linings, Flow Turbulence and Combustion, 70, 69-88.